

See discussions, stats, and author profiles for this publication at: <https://www.researchgate.net/publication/230788915>

# Development and Assessment of a Digital Stereo Photogrammetric System to Measure Cetaceans at Sea

Article in Photogrammetric Engineering and Remote Sensing · March 2012

DOI: 10.14358/PERS.78.3.237

---

CITATIONS

7

READS

336

3 authors, including:



Abraham Growcott  
Ministry for Primary Industries

10 PUBLICATIONS 121 CITATIONS

[SEE PROFILE](#)

Some of the authors of this publication are also working on these related projects:



Marine Biosecurity Toolbox [View project](#)

# Development and Assessment of a Digital Stereo Photogrammetric System to Measure Cetaceans at Sea

Abraham Growcott, Pascal Sirguey, and Stephen M. Dawson

## Abstract

A boat-based digital photogrammetric system has been designed, calibrated, and assessed for the purpose of measuring free ranging sperm whales. A first experiment quantified the effect of the geometry between the target and the stereo system on measurement accuracy. A second experiment tested the robustness of the camera mounting system. Conjugate points in the stereo images were measured using two methods: (a) using an automated centroid detection method, and (b) a manual measurement method to replicate real field conditions. The first experiment demonstrated that a relative error of less than 1 percent could be achieved. The second experiment showed that remounting the two cameras on the stereo bar contributed significantly to measurement error. Nevertheless, the error associated with remounting the cameras compares with that associated with the uncertainties of manually selecting conjugate points. Thus, it is demonstrated that dismounting the stereo system for practical reasons while at sea does not compromise the accuracy.

## Introduction

Photogrammetry has proven to be a useful technique to remotely estimate the size of free-ranging cetacean species (Dawson *et al.*, 1995; Perryman and Westlake, 1998; Spitz *et al.*, 2000; Perryman and Lynn, 2002; Jaquet, 2006). Knowing the length of individuals can allow inference on gender, age, or level of physical/sexual maturity (Dawson *et al.*, 1995; Rhinelander and Dawson, 2004; Jaquet, 2006). In the case of exploited and/or endangered species, such information is valuable in determining the vital rates of the population in question. Three main photogrammetric techniques have been developed to estimate the size of individuals from one or more photographs taken in the field. First, a single image can be used in which an object of known size is visible at the same distance as the individual to provide a scale (e.g., Durban and Parsons, 2006). Alternatively, the size of the individual can be estimated from a single image along with a range measurement (e.g., Perryman and Lynn, 1993). Finally, stereo images from two cameras enable space intersection to be computed between conjugate image points. Thus, the 3-dimensional (3D) coordinates of points that are visible in each image forming the stereo pair can be found in object space and distances between them can be determined (e.g., Dawson *et al.*, 1995).

---

Abraham Growcott and Stephen M. Dawson are with the Department of Marine Science, University of Otago, P.O. Box 56, Dunedin, New Zealand (abegrowcott@hotmail.com).

Pascal Sirguey is with the School of Surveying, University of Otago, P.O. Box 56, Dunedin, New Zealand.

In the context of measuring cetacean size with photogrammetric techniques, studies have used both single and stereo imaging protocols. For example, Rowe and Dawson (2008) projected parallel laser beams with a known baseline onto the dorsal fin of bottlenose dolphins while taking photographs. Thus, the laser dots visible in the photos at a known distance apart provided a scale allowing the size of the fin to be determined. Perryman and Lynn (2002) captured vertical aerial photographs of grey whales using a reconnaissance camera with a fixed focal length. A radar altimeter provided the range to the whale, thus permitting whale sizes to be estimated. With two or more overlapping images, close-range photogrammetric techniques take advantage of the multiple vantage points to allow reconstruction of a 3D model of the object using space intersection of conjugate light rays. For moving targets in wildlife studies, the images must be captured simultaneously. Thus, conventional stereo systems often consist of two cameras mounted onto a rigid body. The latter provides a fixed and known baseline, while images from each camera are captured with overlapping field of views. This technique has been used successfully to measure Hector's dolphins (Bräger and Chong, 1999), bottlenose dolphins (Chong and Schneider, 2001), bowhead whales (Cubbage and Calambokidis, 1987), fin whales (Ratnaswamy and Winn, 1993), and sperm whales (Dawson *et al.*, 1995; Rhinelander and Dawson, 2004). The use of stereo imaging systems underwater, based on still or video cameras, has also proven successful to obtain measurements of marine wildlife (e.g., Klimley and Brown, 1983; Spitz *et al.*, 2000; Shortis *et al.*, 2009).

In the context of sperm whales, four studies have involved boat-based photogrammetry to estimate length. From a known height up the mast of his research vessel, Gordon (1990) took photographs of whales at the surface while they were parallel to the boat. The angle between the horizon and the whale was measured on the developed film and the range was estimated from the curvature of the earth. Jaquet (2006) measured the fluke width of diving sperm whales from digital images which had accompanying range data from a laser rangefinder. She then estimated the total length from the fluke width using a regression relationship calculated from whaling and stranding data. Dawson *et al.* (1995) and Rhinelander and Dawson (2004) used a boat-based stereo camera system to measure the distance between the blowhole and posterior emargination of the dorsal fin of

sperm whales at Kaikoura, New Zealand. Two non-metric film cameras were attached to an aluminium bar to maintain a constant base separation and activated using a paired air release. The total length was then obtained from body proportion measurements derived from whaling records.

The relatively simple system developed by Dawson *et al.* (1995) and subsequently used by Rhinelander and Dawson (2004) was found particularly competitive for measuring the whale's total length. Indeed, the mean coefficients of variation (cv) for both studies were 4.4 percent and 3.1 percent, respectively. This was substantially smaller than the cv of 5.1 percent obtained by Gordon (1990). Jaquet (2006), however, obtained a cv of 1.3 percent based on repeat measurements of fluke width. Nevertheless, the method used by Jaquet (2006) is more prone to error in extrapolation to total length, because the relationship between the total length and fluke width is much weaker ( $R^2 = 0.87$ ; Jaquet, 2006) than the relationship between blow-hole to dorsal fin and total length ( $R^2 = 0.97$ ; Best, 1990). For this reason, the general approach of Dawson *et al.* (1995) appears more desirable. It has the potential to provide a simple and accurate way to measure the length of sperm whales using a boat as a research platform.

Nevertheless, the system designed by Dawson *et al.* (1995) had several flaws making it impractical today. It was film-based, and relied on an analogue stereo plotter, which is a complex, expensive, and now an obsolete piece of equipment. In order to obtain a measurement from each stereo pair, the relative orientation of the two frames had to be determined empirically. Thus, the cost, technical knowledge, and time requirement needed to use and implement stereo photogrammetry limited its application by other researchers. In addition, the measurement accuracy of this analogue system was compromised by an incomplete internal calibration procedure in which only the focal length of each lens was measured. Additional internal orientation parameters such as the position of the principal point of autocollimation (PPA) with respect to the center of the frame and the lens radial distortion were ignored. These parameters are important for modeling the space intersection of light rays originating from conjugate points identified in each frame of a stereo pair (Mikhail *et al.*, 2001, Chapter 3). Despite satisfactory overall performance, Dawson *et al.* (1995) showed that the accuracy of the system decreased substantially as the angle between the optical axis of the cameras and the object photographed departed from a right angle. Although this

effect was predictable due to the worsening of the geometry between the stereo system and the object, its severity could be partly attributed to the propagation of errors due to limited internal calibration of the cameras (Kraus, 1993). Other limitations were that the shutter activation of the two cameras was at times asynchronous, and the need to manually advance the films limited the number of stereo pairs that could be captured per encounter.

Progress in digital camera and computer technology now enables the close range photogrammetry problem to be fully digital (Mikhail *et al.*, 2001). Analytical processing, whereby a fully deterministic mathematical solution is found for the photogrammetric problem, can now be readily implemented with standard off-the-shelf digital cameras. This enables many of the shortcomings associated with the analog stereo system and analog processing to be overcome. This study reports on the design of a digital stereo photogrammetric system for measurement of sperm whales, its calibration, and accuracy assessment.

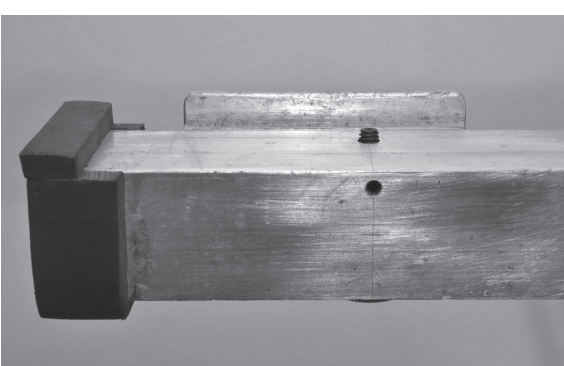
## Methods

### Digital Stereo Camera System

The stereo photogrammetric system designed in this study is a modification of that designed by Dawson *et al.* (1995). It is based on a 2.56 meter aluminum bar of rectangular section (50 mm × 40 mm; wall thickness 2.5 mm). On each side, the camera mounting system consisted of butt plates to the rear locating the camera bodies while fastened by a thumbscrew (Figure 1). The original analog film cameras and air release trigger have been replaced by two Nikon D70s single-lens reflex (SLR) digital cameras (six megapixel CCD sensor) equipped with AF Nikkor 50 mm f/1.8D lenses and a custom-built electronic remote trigger. The lenses were set to manual focus, and their focusing rings taped in place at infinity focus to maintain a constant interior orientation. In the field, the cameras were set to 400 ISO, shutter priority automatic exposure, with shutter speeds fixed at 1/1250<sup>th</sup> of a second to minimize motion blur. In the field, natural light was sufficient to ensure acceptable depth of field from around 30 m to infinity. During indoor calibration, the aperture was closed to f/22 to bring the near limit of acceptable sharpness at 5.5 meters. Figure 2 shows a stereo pair of a sperm whale captured by the system once operational to illustrate the points being measured during operational use.



(a)



(b)

Figure 1. (a) the stereo-camera system in use, and (b) close-up showing the camera mounting system with the rear butt plate and thumbscrew controlling the position and alignment of the camera.

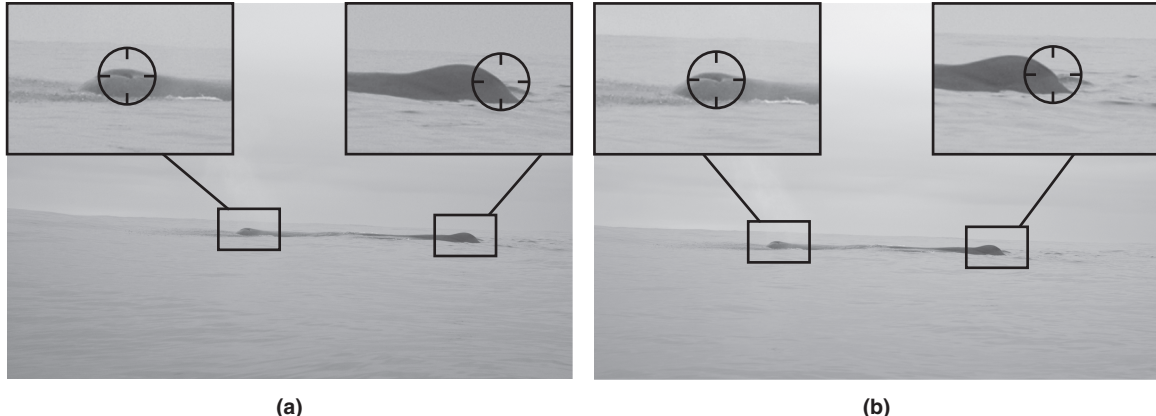


Figure 2. Example of a stereo pair: (a) left image and (b) right image captured by the system once operational. The close-up views show the measurement points on the sperm whale, specifically the blowhole and posterior emargination of the dorsal fin.

In the context of photogrammetry, several parameters must be determined to measure accurately the length of objects from stereo photographs. One set of parameters known as Interior Orientation Parameters (IOPs) relates to the geometrical properties of the lens. They involve the precise focal length, the position of the PPA with respect to the center of frame, the radial/tangential distortion profile of the lens (see Brown, 1971), sometimes supplemented by additional affinity parameters to accommodate distortions inherent to the CCD sensor (e.g., Fraser, 1997). When two cameras are linked to form a stereo system, parameters known as Relative Orientation Parameters (ROPs) summarize the precise position and orientation of the cameras to each other (Lerma *et al.*, 2010). As illustrated in Figure 3, the ROPS account for six parameters:

1. three parameters describing the translations of one camera with respect to the other ( $b_x$ ,  $b_y$ ,  $b_z$ ), and
2. three parameters describing the orientation angles of one camera with respect to the other ( $\varphi$ ,  $\theta$ ,  $\omega$ ).

The topic of calibration of cameras, as well as calibration of stereo systems is well addressed in general photogrammetric textbooks (e.g., Kraus, 1993 and 1997; Mikhail *et al.*, 2001), and an extensive body of literature documents specifically the calibration of close-range cameras (e.g., Brown, 1971; Clarke and Fryer, 1998; Luhmann, 2006). In particular, IOPs and ROPS can be estimated by performing an indoor calibration procedure using close range photogrammetric software (Fraser, 1997; Fraser and Edmundson, 2000). Note that the sequence of rotations illustrated in Figure 3 and used throughout this article (i.e., a positive rotation of angle  $\varphi$  around the z axis followed by a positive rotation of angle  $\theta$  around the x axis, and finally a negative rotation of angle  $\omega$  around the y axis) departs from most photogrammetric textbooks and is specific to the close range photogrammetric software used in this study (*Australis* software).

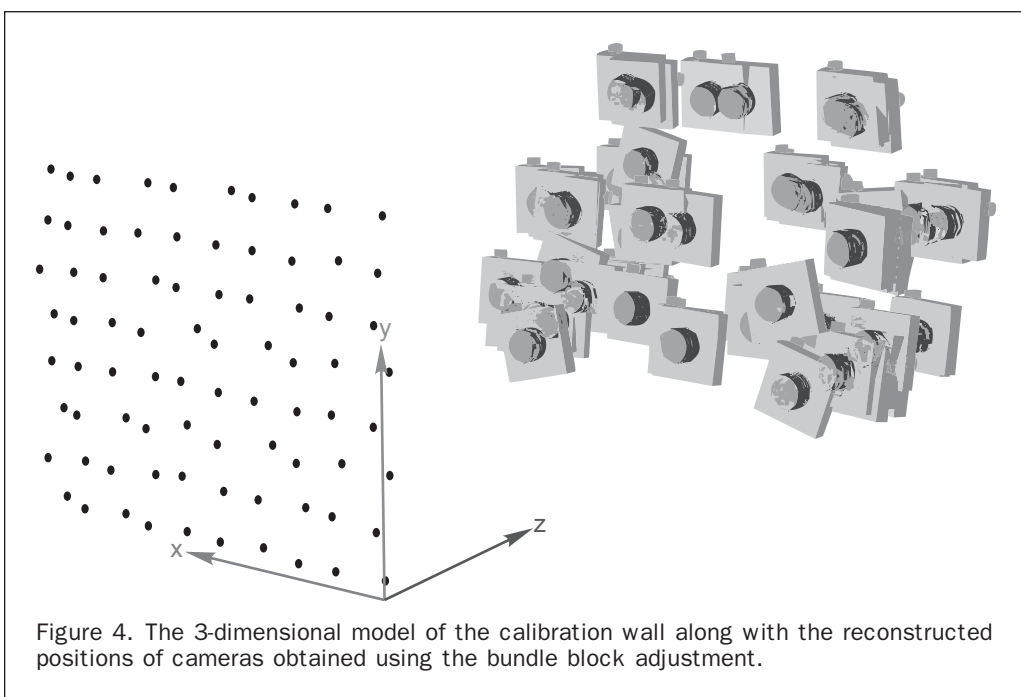
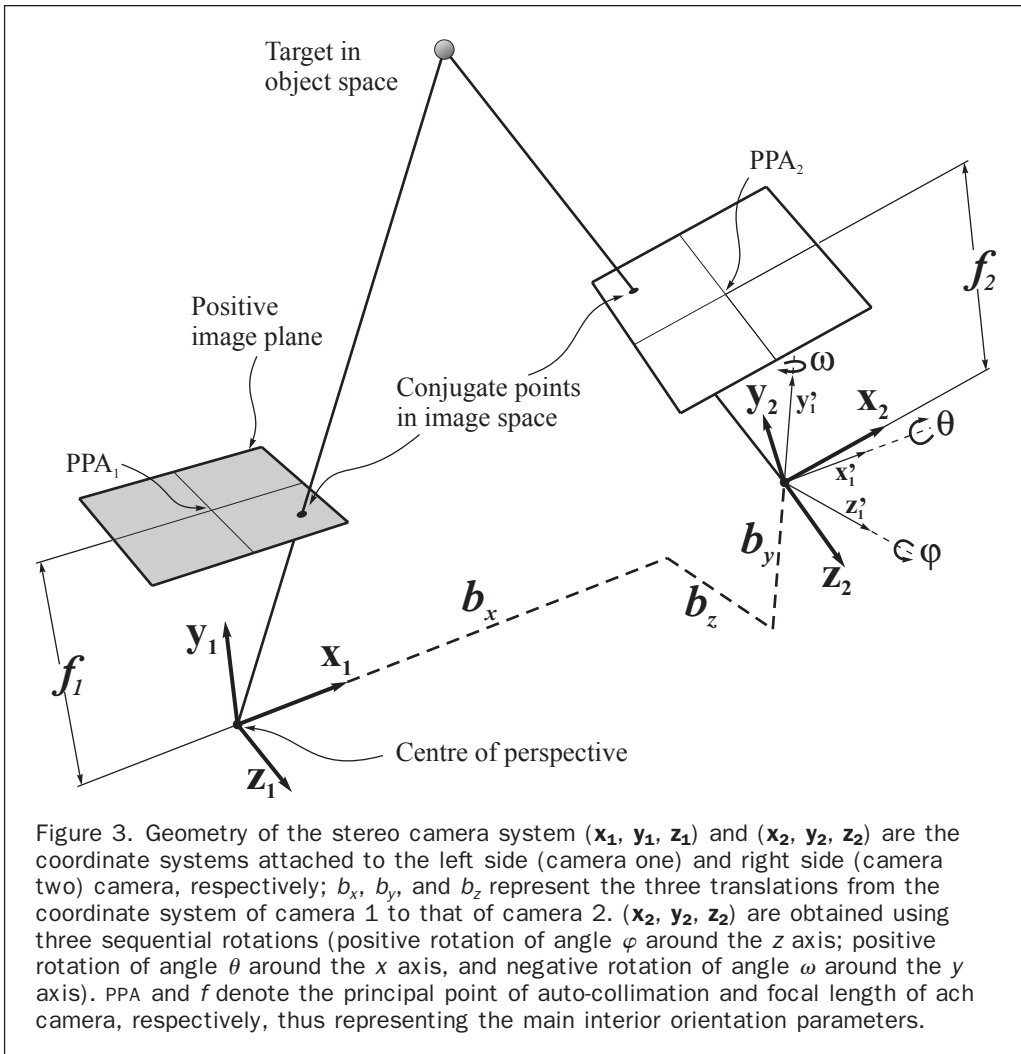
#### Calibration using *Australis*

The close range photogrammetric software *Australis* (version 6.01, Photometrix Pty, Ltd, Australia; see Fraser, 1997; Fraser and Edmundson, 2000) was used to determine the IOPs of each camera, as well as to derive indirectly the ROPS associated with the rigid mount of the stereo system. A field calibration strategy was used whereby stereo pairs of an

indoor calibration wall were captured from various vantage points and orientations. The calibration wall consists of a 3D array of 80 fixed reference targets whose positions are precisely known (the coordinates have a root-mean-square value of 0.05 mm; see Chong and Schneider, 2001). The targets are white circular retro-reflective surfaces on a black background. *Australis* has the capability of locating and labeling automatically the centroid of such round and highly contrasting targets using least-squares template matching of elliptical targets (Fraser and Edmundson, 2000). This feature enables measurements of points to be automatically obtained with sub-pixel accuracy (Clarke *et al.*, 1993).

However, the *Australis* software is limited in the sense that it cannot readily accommodate a stereo configuration. In other words, the *Australis* software does not allow baseline distance constraints to be defined when calibrating multiple cameras (e.g., Lerma *et al.*, 2010). Instead, all individual frames used for camera calibration are assumed to be independent. The position and attitude of the camera for each frame are thus determined with respect to the reference framework of the targets (i.e., attached to the calibration wall), hence exterior to the stereo system. These orientation parameters (i.e., the three translations and the three rotations) obtained from *Australis* are thus referred here as Exterior Orientation Parameters (EOPs). The IOPs for each camera as well as the EOPs for each single image were computed in *Australis* by means of a bundle block adjustment. This process estimates simultaneously all unknown parameters using an iterative least squares solution of the linearized form of the co-linearity equations (Mikhail *et al.*, 2001, Chapter 9). Figure 4 illustrates the exposure stations of 64 images of the calibration wall determined after bundle block adjustment.

Once the EOPs of two images forming a stereo pair are determined in *Australis* by means of bundle block adjustment, it becomes relatively simple to obtain the ROPS by reducing the position and orientation of each frame so that the new reference framework is attached to the left camera. This method, used by Harvey and Shortis (1998), has the effect of setting the coordinates of the perspective center of the first camera to null values, as well as its attitude angles. In turn, the transformed EOPs of the frame corresponding to the right camera become estimates of the ROPS. Due to the non conventional sequence of rotations in *Australis*, the general form of the rotation matrix is



$$\mathbf{R} = \begin{bmatrix} \cos\varphi \cos\omega + \sin\varphi \sin\theta \sin\omega & \cos\theta \sin\omega \\ -\sin\varphi \cos\theta & \sin\theta \\ -\cos\varphi \sin\omega + \sin\varphi \sin\theta \cos\omega & \cos\theta \cos\omega \end{bmatrix}. \quad (1)$$

The translation vector  $\mathbf{t}_{\text{rel}}$  corresponding to the position of the right camera relative to the left one can be obtained from the coordinate transformation by

$$\mathbf{t}_{\text{rel}} = \mathbf{R}_1(\mathbf{t}_2 - \mathbf{t}_1), \quad (2)$$

where  $\mathbf{t}_1$  and  $\mathbf{t}_2$  are the vectors of translation expressing the position of the left and right frame of a stereo pair, respectively, with respect to the wall as obtained in *Australis*.  $\mathbf{R}_1$  and  $\mathbf{R}_2$  are the rotations matrices associated with the attitude parameters with respect to the wall obtained in *Australis*. The orientation of the right camera relative to the left is found by deriving the three elementary rotation angles from

$$\mathbf{t}_{\text{rel}} = (\mathbf{R}_1 \mathbf{R}_2^{-1})^{-1}. \quad (3)$$

The calibration process was completed by first capturing 25 photos of the calibration wall with each camera. Each of these 50 photos was captured from various positions and orientations, although constrained by the size of the calibration room and the minimum distance of acceptable sharpness (5.5 m). Within the acceptable range, the calibration wall was photographed in a convergent manner from various distances, angles, and with the cameras rolled on their axis in order to achieve strong imaging geometry (Brown, 1989). This enabled a robust estimation of the parameters, while minimizing the problem of correlation between IOPs and EOPs (Mikhail *et al.*, 2001, pp. 259). Then, each camera was attached to the stereo bar and seven stereo pairs of the calibration wall were captured with the system placed at different distances, height, and angles. The cameras were then taken off the stereo bar and remounted to capture another set of seven stereo pairs. This procedure was repeated to obtain three independent sets of seven stereo pairs. The purpose of this protocol was to investigate the robustness of the relative orientation enforced by the bar with respect to mounting and dismounting the cameras. Thus, this procedure simulated the fact that, each day on the boat, the cameras are mounted on the bar once on site and removed before going back to shore due to practical reasons associated with handling the system and cameras on a relatively small boat in a maritime environment.

Only a limited number of stereo pairs could be taken due to the length of the stereo bar (i.e., 2.5 m) being relatively large compared to the calibration room. This also complicated the capture of sufficiently convergent and rolled frames in order to fulfill the recommended configurations for the calibration of close-range photogrammetric systems (Brown, 1989). The additional 25 images captured independently by each stand-alone camera provided the redundancy and rotations required to allow a more accurate and robust determination of the IOPs and EOPs of each camera. The final ROPS of the stereo system (i.e., the translation vector and rotation matrix of the right camera with respect to the left) were obtained by averaging the individual ROPS obtained from the three sets of seven stereo pairs.

### Field Testing of the Calibrated Digital Stereo System

In order to assess the robustness and accuracy of the calibrated stereo system, a field experiment was conducted. The experiment had four main purposes:

1. to test whether the calibration of the digital stereo system obtained indoor (i.e., IOPS for each camera and ROPS for the stereo system) allows accurate measurements in the field,
2. to investigate the effect of distance and angle of view between the stereo system and the target in order to assess how non-ideal geometry affected measurement accuracy (Harvey *et al.*, 2010),
3. to assess how dismounting and remounting the cameras onto the bar affected measurement accuracy, and
4. to assess how the manual measurement of conjugate points on the stereo pairs, as interpreted by a user, affected accuracy.

The experiment was conducted on a sports field. In order to replicate exactly how sperm whales would be measured in real conditions, five images of a blowhole and five of a dorsal fin printed at life-size were attached to a fence at five different distances (approximately 4, 6, 8, 10, and 12 meters apart; note that the distance between the blowhole and dorsal fin from whales measured at Kaikoura is approximately 7.5 to 10 meters (Dawson *et al.*, 1995; Rhineland and Dawson, 2004)). The measured distances were chosen to encompass the likely whale size that this project would encounter. Directly beneath each of these photographs, a white circle of 10 cm in diameter was taped onto a black background to enable automatic point measurement in *Australis*. Reference distances between the targets  $d_{\text{ref}}$  were obtained by averaging ten samples collected with a measuring tape (the standard deviation (SD) ranged from 1 to 5 cm depending on the targets being 4 to 12 meters apart, respectively).

A network consisting of four distances from the fence (40, 50, 60, 70 meters) and seven angles ( $-30^\circ, -20^\circ, -10^\circ, 0^\circ, 10^\circ, 20^\circ, 30^\circ$  degrees; see Figure 5) was constructed using a total station (Nikon NPL-362) and a corner reflector. Each position once found was marked in the ground with a wooden peg. Within this framework two separate experiments were conducted:

1. One stereo pair was captured at each of the 28 locations to test the effect that distance and angle between the system and the target had on measurement error.
2. Ten stereo pairs were taken at three positions of the network, with the cameras being dismounted then remounted on the stereo bar between each exposure. This second experiment aimed at quantifying the error associated with removing and remounting the cameras on the stereo bar. The three positions in the network were chosen to represent the worst geometry whereby the parallax is minimized ( $-30^\circ, 70$  m), the best geometry whereby the parallax is maximized ( $0^\circ, 40$  m), and an intermediate geometry at close distance but severe angle ( $-30^\circ, 40$ m).

*Australis* was also used to measure the positions and dimensions of objects using triangulation of conjugate points identified in orientated stereo pairs. For each experiment, two methods of measurement were conducted in *Australis*. First, the automatic centroid detection feature was used to determine automatically the position of the center of the white circle with sub-pixel accuracy. This method allowed the optimum performance of the stereo system to be tested, without the user potentially introducing uncertainties and bias when interpreting the position of conjugate points in the stereo pairs. Second, the user measured manually the conjugate locations of the blowhole and the dorsal fin printed on the boards to enable the assessment of human error. Each measurement was repeated three times to allow calculation of variance associated with the mean estimated distance  $d_{\text{est}}$ .

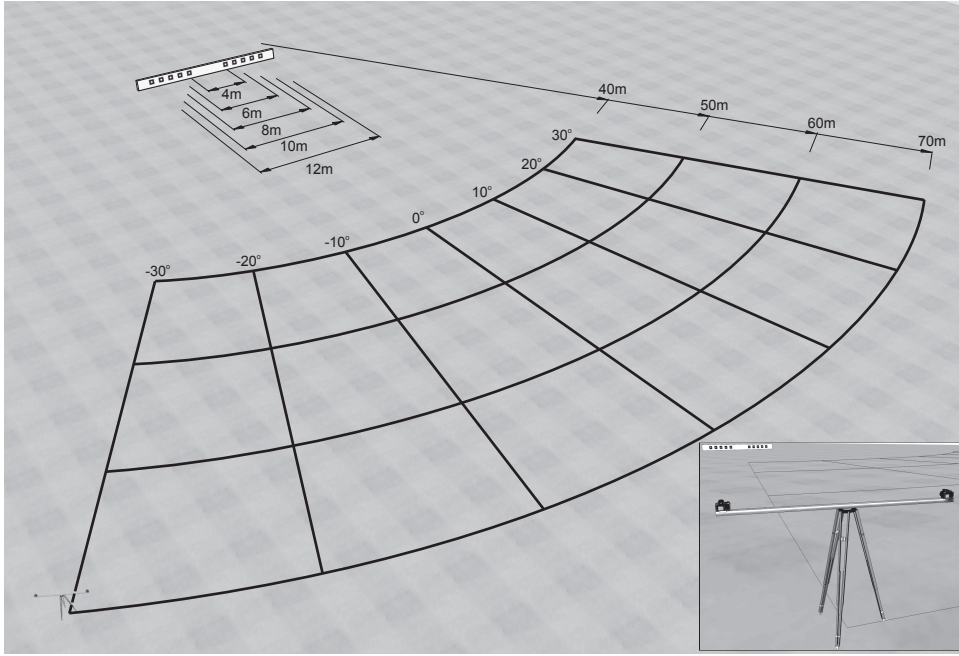


Figure 5. The assessment network showing the four distances (i.e., 40, 50, 60, 70 meters) and seven angles (i.e.,  $-30^\circ$ ,  $-20^\circ$ ,  $-10^\circ$ ,  $0^\circ$ ,  $10^\circ$ ,  $20^\circ$ ,  $30^\circ$ ) from where the stereo pairs were captured, as well as the position of the targets and the measured distances (i.e., 4, 6, 8, 10, 12 meters).

## Results

The calibrated IOPs of each camera along with their SD are provided in Table 1. They relate to the camera calibration model described by Fraser (1997). The averaged values and SD of the ROPS obtained during indoor calibration are shown in Table 2. In the context of an indirect estimation of the ROPS, the values of SD associated with the ROPS estimates compare to those reported by Harvey and Shortis (1998) in a similar calibration protocol.

Following the field experiment, the relative error of measurement was computed for each target as  $\varepsilon\% =$

$(d_{\text{est}} - d_{\text{ref}})/d_{\text{ref}}$ . The relative error of measurement over the entire network is shown for automatic and manual measurement methods for two measured lengths, 8 meters and 10 meters (Figure 6). Only two measured distances are shown because the pattern was similar over all other measured distances. The overall performance of the system was assessed using the mean relative error and associated SD, as well as the Root Mean Relative Square Error ( $\text{RMRSE} = \sqrt{\sum \varepsilon^2\% / n}$  because, similarly to its counterpart the Root Mean Square Error (RMSE), it accounts simultaneously for both the bias (accuracy) and the

TABLE 1. CALIBRATED VALUES AND STANDARD DEVIATION OF THE INTERIOR ORIENTATION PARAMETERS DEFINED IN AUSTRALIS (SEE FRASER, 1997)

	Left camera		Right camera	
	value	SD	value	SD
<i>camera interior orientation</i>				
focal length [mm]	52.8882	$3.04 \times 10^{-3}$	52.8824	$1.00 \times 10^{-4}$
$x_p$ [mm]	0.0225	$2.62 \times 10^{-3}$	0.0098	$4.00 \times 10^{-4}$
$y_p$ [mm]	-0.0580	$1.15 \times 10^{-3}$	0.0504	$1.41 \times 10^{-3}$
<i>radial distortion parameters</i>				
$k_1$ [ $\text{mm}^{-2}$ ]	$3.909 \times 10^{-6}$	$5.62 \times 10^{-7}$	$6.851 \times 10^{-6}$	$1.46 \times 10^{-7}$
$k_2$ [ $\text{mm}^{-4}$ ]	$2.266 \times 10^{-8}$	$6.64 \times 10^{-9}$	$-5.836 \times 10^{-11}$	$1.14 \times 10^{-9}$
$k_3$ [ $\text{mm}^{-6}$ ]	$-6.981 \times 10^{-11}$	$2.31 \times 10^{-11}$	$-7.270 \times 10^{-12}$	$8.38 \times 10^{-12}$
<i>decentring distortion parameters</i>				
$p_1$ [ $\text{mm}^{-1}$ ]	$-1.228 \times 10^{-5}$	$3.49 \times 10^{-7}$	$-1.665 \times 10^{-5}$	$5.02 \times 10^{-7}$
$p_2$ [ $\text{mm}^{-1}$ ]	$-9.375 \times 10^{-7}$	$1.53 \times 10^{-7}$	$-2.970 \times 10^{-6}$	$2.56 \times 10^{-7}$
<i>affinity, non-orthogonality parameters</i>				
$b_1$ [unitless]	$-3.100 \times 10^{-5}$	$1.68 \times 10^{-6}$	$1.257 \times 10^{-5}$	$4.82 \times 10^{-6}$
$b_2$ [unitless]	$-5.669 \times 10^{-5}$	$1.06 \times 10^{-6}$	$5.782 \times 10^{-5}$	$2.37 \times 10^{-6}$

TABLE 2. AVERAGE VALUE AND STANDARD DEVIATION OF THE RELATIVE ORIENTATION PARAMETERS  
(THE LEFT CAMERA IS USED AS ORIGIN)

	$b_x$ [mm]	$b_y$ [mm]	$b_z$ [mm]	$\varphi$ [deg]	$\theta$ [deg]	$\omega$ [deg]
Mean	2398.041	11.402	-2.647	0.424	0.726	-0.145
Standard deviation	2.601	0.948	2.643	0.019	0.029	0.080

SD (precision) of the relative error (Willmott *et al.*, 1985). Over the distance/angle network, the manual measurement method yielded a mean measurement error of 0.57 percent ( $SD = 1.10\%$ , RMRSE = 1.24%). In contrast, the mean measurement error when investigating the automatic measurement method was 0.36 percent ( $SD = 0.47\%$ , RMRSE = 0.60%). The automatic measurement method is substantially less variable than the manual method because it involves a deterministic and therefore repeatable technique.

A general linear model (multi-way analysis of variance) showed that the variance in the measurements is significantly influenced by a number of factors (Table 3). The factor explaining most of the variance of the error was the measurement method used ( $F$ -value = 81.52,  $p < 0.001$ ). The angle at which the photo was captured came second ( $F$ -value = 20.99,  $p < 0.001$ ), followed by the interaction effect between the measurement method and the angle ( $F$ -value = 13.26,  $p < 0.001$ ). The distance between the system and the target also explained a significant amount of measurement errors ( $F$ -value = 10.51,  $p < 0.001$ ). Finally, the length between targets on the fence (i.e., wall distance) contributed significantly but to a lower extent to the measurement error ( $F$ -value = 7.08,  $p < 0.001$ ).

From the second experiment, the relative error associated with the remounting of the two cameras between exposures is shown in Figure 7. The relative errors ( $\varepsilon\%$ ) originating from the manual selection of conjugate points were calculated for each of the five reference distances in the ten stereo pairs ( $n = 50$ ). The RMRSE was 0.76 percent at the best geometry ( $0^\circ, 40$  m), 0.80 percent at intermediate geometry (i.e.,  $30^\circ, 40$  m), and 2.1 percent at the worst geometry ( $0^\circ, 70$  m).

Again, a multi-way analysis of variance was used to identify the factors which contributed most to the variance of measurement error (Table 4). The variance in the measurements was significantly influenced by three factors. The position at which the stereo pairs were captured appeared to explain most of the variance ( $F$ -value = 62.72,  $p < 0.001$ ). The method used to measure the photographs came second ( $F$ -value = 16.57,  $p < 0.001$ ). Finally, the interaction between position and method came third ( $F$ -value = 8.54,  $p < 0.001$ ).

Because the two experiments were conducted independently, it was not readily possible to discriminate directly whether the relative geometry between the stereo system and the target (i.e., the distance and angle at which the picture was captured) or the process of dismounting and remounting

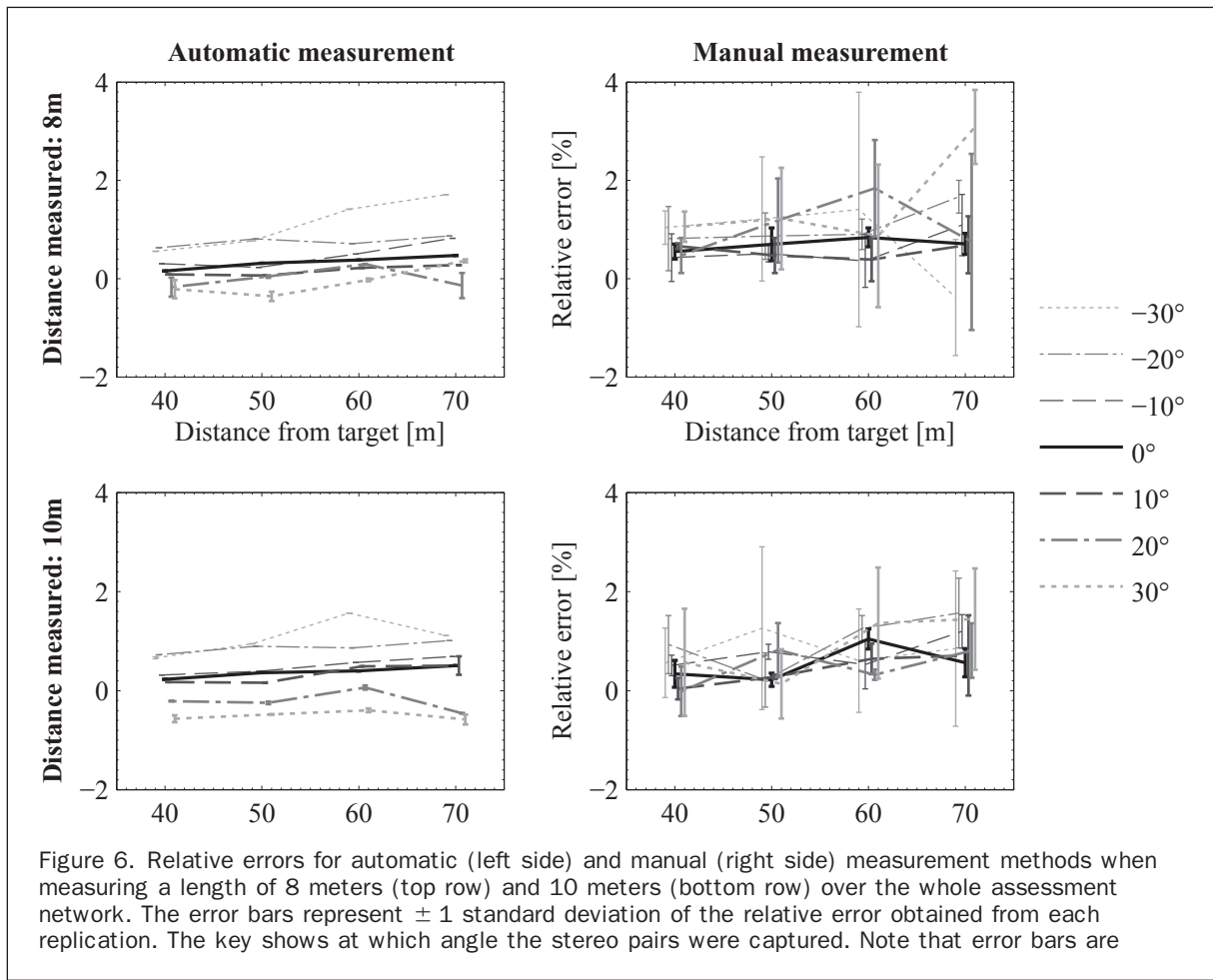


Figure 6. Relative errors for automatic (left side) and manual (right side) measurement methods when measuring a length of 8 meters (top row) and 10 meters (bottom row) over the whole assessment network. The error bars represent  $\pm 1$  standard deviation of the relative error obtained from each replication. The key shows at which angle the stereo pairs were captured. Note that error bars are

TABLE 3. RESULTS OF THE GENERAL LINEAR MODEL APPLIED TO THE DISTANCE/ANGLE FIELD EXPERIMENT. THE SOURCES OF ERROR ARE ARRANGED BY F-VALUES (HIGHEST TO LOWEST); D.F. = DEGREES OF FREEDOM

Source	d.f.	F-value	p-value
Method	1	81.52	<0.001
Angle	6	20.99	<0.001
Method*angle	6	13.26	<0.001
Distance	3	10.51	<0.001
Wall distance	4	7.08	<0.001
Wall distance*method	4	2.87	0.029
Wall distance*angle	24	2.47	0.002
Wall*method*angle	24	2.44	0.002
Angle*distance	18	2.01	0.020
Method*angle*distance	18	1.78	0.045
Wall distance*method*distance	12	1.09	0.385
Wall distance*angle*distance	72	1.08	0.379
Wall distance*distance	12	0.99	0.463
Method*distance	3	0.20	0.896

the cameras between exposures influenced the error the most. However, comparison of relative errors from both experiments (Figure 8) reveals that remounting the cameras introduced more variability in measurements and that this variability increased as the geometry with respect to the target worsens.

When using the digital stereo system in the field to measure sperm whales, only the manual measurement method can be used. Thus, both experiments were also compared with respect to distances obtained from manual measurements. Figure 9 demonstrates that there is a considerable overlap in error bars for all but one measured distance.

## Discussion

The indoor calibration of the digital stereo system facilitated the estimation of both the IOPS and ROPS. The SD associated with each ROP was considered small enough (see Table 2) to justify that the mean values of ROPS obtained from each separate mount could be considered robust enough for use.

To further examine the suitability of the ROPS, an outdoor experiment was conducted. This included measuring a range of targets of known length at a variety of distances and angles, in a protocol that replicated what would occur in the field. The angle and distance at which stereo pairs were captured explained a significant amount of measurement uncertainty. Nevertheless, the manual selection of conjugate points in the stereo pairs appeared to

contribute more to measurement uncertainty. The automatic measurement method is able to locate the centroid of the image of high contrast circular targets to sub-pixel accuracy, resulting in minimal variation between repeated measurements of the same stereo pair. The manual selection of conjugate points is influenced by human interpretation, which inherently compromises the repeatability of the process (Dawson *et al.*, 1995).

The second experiment tested the effect that removing and remounting the cameras had on measurement error over three positions (40 m – 0°, 40 m – 30°, and 70 m – 30°). The position from where the stereo pairs were captured explained most of the measurement uncertainty. As the geometry between the stereo system and the target worsens (i.e., distance and/or absolute angle increasing), the base-height ratio associated with the stereo-system decreases (i.e., the baseline remains the same while the distance to the target increases), resulting in a decrease in measurement accuracy. In addition, at further distance the spatial resolution becomes coarser, complicating the measurement of conjugate points. On the other hand, the manual selection of conjugate points also explained a significant proportion of measurement uncertainty.

Although these factors were not combined in a single experiment, the errors associated with the manual identification of the blowhole and posterior emargination of the dorsal fin (i.e., the user error) are comparable to those associated with the process of remounting the cameras on the stereo bar between trials. Thus, the ROPS determined during the indoor calibration of the system are confirmed to be robust enough for measuring whales at sea. Moreover, the processes of visual interpretation of conjugate points and remounting of the cameras are independent. Therefore, the error associated with the first process has no effect on that

TABLE 4. RESULTS FROM THE GENERAL LINEAR MODEL APPLIED TO THE REMOUNTING EXPERIMENT. THE SOURCES OF ERROR ARE ARRANGED BY F-VALUE; D.F. = DEGREES OF FREEDOM.

Source	d.f.	F-value	p-value
Position	2	62.72	<0.001
Method	1	16.57	<0.001
Position*Method	2	8.54	<0.001
Wall distance*Method	4	2.20	0.070
Position*Wall distance	8	1.98	0.049
Wall distance	4	1.48	0.208
Position*Wall distance*Method	8	0.98	0.449

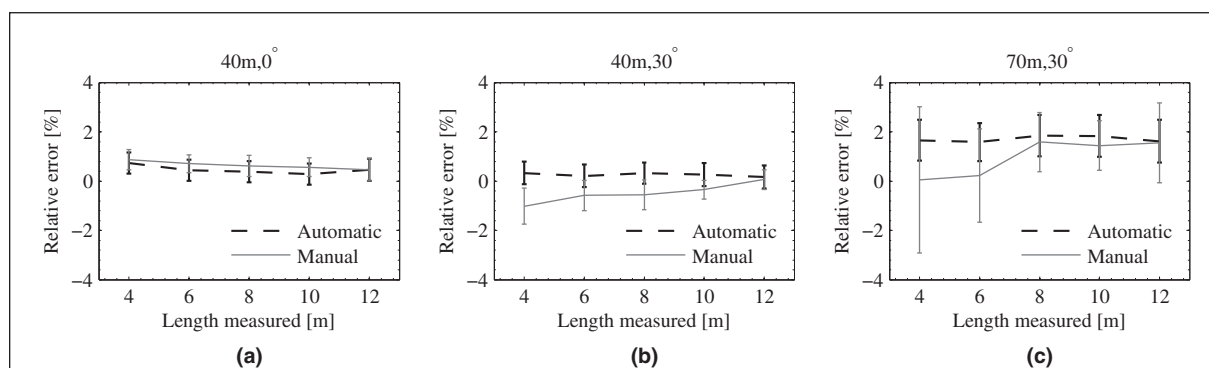


Figure 7. Relative error for the experiment that involved remounting the cameras between each exposure (ten replications for each position). Two measurement methods are compared (i.e., automatic and manual). The stereo pairs processed for the (a), (b), and (c) graphs were captured from positions 40 m-0°, 40 m-30°, 70 m-0°, respectively. The error bars represents  $\pm 1$  standard deviation.

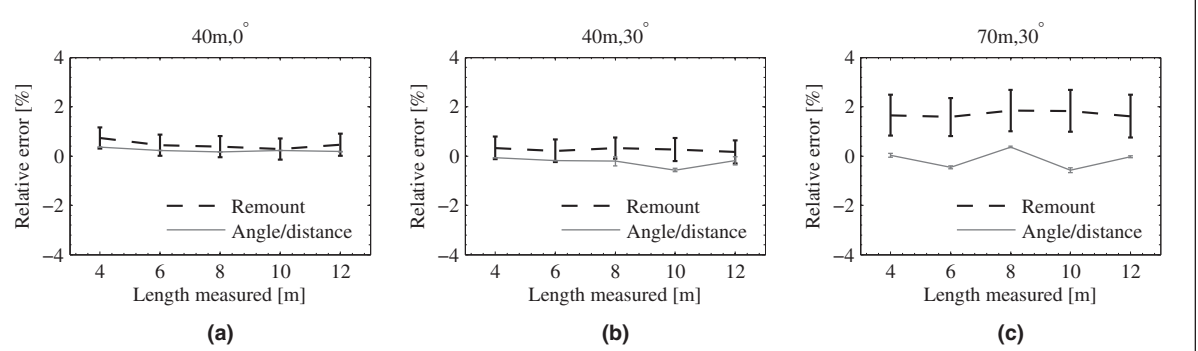


Figure 8. Comparison of relative error for the corresponding positions of both experiments (automatic measurement method only). The (a), (b), and (c) graphs correspond to stereo pairs captured from positions 40 m-0°, 40 m-30°, 70 m-0°, respectively. The error bars represents  $\pm 1$  standard deviation.

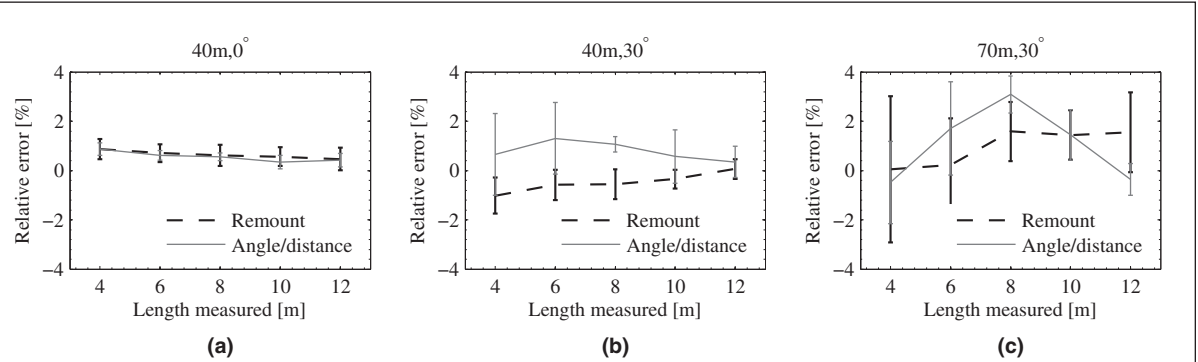


Figure 9. Comparison of relative error for the corresponding positions of both experiments (manual measurement method only). The (a), (b), and (c) graphs correspond to stereo pairs captured from positions 40 m-0°, 40 m-30°, 70 m-0°, respectively. The error bars represents  $\pm 1$  standard deviation.

introduced by the other. Recalibration of the stereo system after remounting the cameras is unnecessary given that the user interpretation of conjugate points will introduce at least as much uncertainty.

The advantage of using two different measurement methods is that the automatic method permitted a deterministic and repeatable measurement of conjugate points, which enables the system to be consistently assessed, while the manual measurement accounts for user bias and interpretation. However, in the field it is only possible to use the manual measurement method. These two experiments have allowed the two measurement methods to be assessed independently. This provided an objective way to quantify the effect that manually selecting conjugate points in the stereo pairs has on measurement error.

It also must be kept in mind that another factor limiting the accuracy of measurements is that sperm whales are inherently flexible (Dawson *et al.*, 1995). Therefore, it is believed that a more accurate system will not necessarily result in a better estimate of whale length.

This new digital stereo system has eliminated many of the shortcomings of the previously used analog system. Further, its measurements of individual whales are much more consistent. Repeated measurements of the same whale at sea show a mean CV of 1.57 percent (Growcott *et al.*, 2011). For the old, analog system this figure was almost three times larger (CV = 4.35%; Dawson *et al.*, 1995). The only specialized item required to design a similar system is the photogrammetry software *Australis* or any alternative but

equivalent package (e.g., *Photomodeller*). This new system proved to be simple to calibrate and to use and provided a simpler and more accurate way to measure the distance between the blowhole and posterior emargination of the dorsal fin of sperm whales. Close-range photogrammetry software such as *Australis* is also very flexible in that a variety of camera sensors and lenses can be calibrated and used to suit the intended application. If designing a similar system for either biological or non-biological purposes, it is expected that the accuracy would be further improved by keeping the cameras permanently mounted on the stereo bar.

## Conclusions

A new fully digital stereo photogrammetry system has been developed, calibrated, and had its measurement accuracy assessed to allow remote measurement of free-ranging sperm whales. The manual selection of the conjugate pixels in the stereo pairs is demonstrated to play a major role in the measurement error. Dismounting and remounting the system obviously introduces also a substantial degree of uncertainty since the calibrated values of the ROPs are assumed constant. It is shown, however, that the errors attributed to the manual selection of points remains comparable to this uncertainty, thereby masking the effect of changes to the relative orientation caused by dismounting and remounting the cameras. This demonstrates that dismounting the stereo system for logistic purposes while at sea does not compromise the accuracy despite the lack of recalibration. The

accuracy of the system when investigating the manual measurement method over the distance/angle network had a mean measurement error of 0.57 percent ( $SD = 1.10\%$ ;  $RMRSE = 1.24\%$ ), and thus is deemed accurate enough for the measurement of sperm whales length given the inherent flexibility of sperm whales when at the surface.

## Acknowledgments

The authors wish to express their gratitude to Brian Niven of the Mathematics & Statistics Department at the University of Otago for his help. This project was conducted with the financial support of the New Zealand Whale and Dolphin Trust.

## References

- Best, P.B., 1990. A note on proportional body measurements in sperm whales, *Report of the International Whaling Commission*, Technical Report SC/42/sp9.
- Bräger, S., and A.K. Chong, 1999. An application of close range photogrammetry in dolphin studies, *The Photogrammetric Record*, 16(93):503–517.
- Brown, D., 1989. A strategy for multi-camera on-the-job self-calibration, *Schriftenreihe 14*, Institut für photogrammetrie der Universität Stuttgart, 302:9–21.
- Brown, D.C., 1971. Close-range camera calibration, *Photogrammetric Engineering*, 37(8):855–866.
- Chong, A.K., and K. Schneider, 2001. Two-medium photogrammetry for bottlenose dolphin studies, *Photogrammetric Engineering & Remote Sensing*, 67(5):621–628.
- Clarke, T.A., M.A.R. Cooper, and J.G. Fryer, 1993. An estimator for the random error in subpixel target location and its use in the bundle adjustment, *Optical 3-D measurements Techniques II*, Wichmann, Karlsruhe, pp. 161–168.
- Clarke, T.A., and J.G. Fryer, 1998. The development of camera calibration methods and models, *The Photogrammetric Record*, 16(91):51–66.
- Cubbage, J.C., and J. Calambokidis, 1987. Size-class segregation of Bowhead whales discerned through aerial stereophotogrammetry, *Marine Mammal Science*, 3(2):179–185.
- Dawson, S.M., C.J. Cheshum, P.J. Hunt, and E. Slooten, 1995. An inexpensive stereophotographic technique to measure sperm whales from small boats, *Report of the International Whaling Commission*, 45:431–436.
- Durban, J.W., and K.M. Parsons, 2006. Laser-metrics of free ranging killer whales, *Marine Mammal Science*, 22(3):735–743.
- Fraser, C.S., 1997. Digital camera self-calibration, *ISPRS Journal of Photogrammetry and Remote Sensing*, 52(4):149–159.
- Fraser, C.S., and K.L. Edmundson, 2000. Design and implementation of a computational processing system for off-line digital close-range photogrammetry, *ISPRS Journal of Photogrammetry and Remote Sensing*, 55(4):94–104.
- Gordon, J.C.D., 1990. A simple photographic technique for measuring the length of whales from boats at sea, *Report of the International Whaling Commission*, 40:581–588.
- Growcott, A., B. Miller, P. Sirguey, E. Slooten, and S. Dawson, 2011. Measuring body length of male sperm whales from their clicks: The relationship between inter-pulse intervals and photogrammetrically measured lengths, *Journal of the Acoustical Society of America*, 130(1):568–573.
- Harvey, E.S., J. Goetze, B. McLaren, T. Langlois, and M.R. Shortis, 2010. The influence of range and image resolution on underwater stereo-video measurement: A comparison of high definition and broadcast resolution video with high, medium and low image compression factors, *Marine Technology Society Journal*, 44(1):75–84.
- Harvey, E.S., and M.R. Shortis, 1998. Calibration stability of an underwater stereo-video system: Implications for measurement accuracy and precision, *Marine Technology Society Journal*, 32(2):3–17.
- Jacquet, N., 2006. A simple photogrammetric technique to measure sperm whale at sea, *Marine Mammal Science*, 22(4):862–879.
- Klimley, A.P., and S.T. Brown, 1983. Stereophotography for the field biologist: measurement of lengths and three-dimensional positions of free-swimming sharks, *Marine Biology*, 74(2):175–185.
- Kraus, K., 1993. *Photogrammetry, Fundamentals and Standard Processes*, Volume 1 of *Photogrammetry*, Ferdinand Dümmlers Verlag, Bonn, Germany, 402 p.
- Kraus, K., 1997. *Photogrammetry, Advanced Methods and Applications*, Volume 2 of *Photogrammetry*, Ferdinand Dümmlers Verlag, Bonn, Germany, 466 p.
- Lerma, J.L., S. Navarro, M. Cabrelles, and A.E. Segu, 2010. Camera calibration with baseline distance constraints, *The Photogrammetric Record*, 25(130):140–158.
- Luhmann, T., 2006. *Close Range Photogrammetry: Principles, Techniques and Applications*, Whittles, Dunbeath, Scotland, 510 p.
- Mikhail, E.M., J.S. Bethel, and J.C. McGlone, 2001. *Introduction to Modern Photogrammetry*, John Wiley & Sons, New York, 479 p.
- Perryman, W.L., and M.S. Lynn, 1993. Identification of geographic forms of common dolphins (*Delphinus delphis*) from aerial photogrammetry, *Marine Mammal Science*, 9(2):119–137.
- Perryman, W.L., and M.S. Lynn, 2002. Evaluation of nutritive condition and reproductive status of migrating gray whales (*Eschrichtius robustus*) based on analysis of photogrammetric data, *Journal of Cetacean Research and Management*, 4(2):155–164.
- Perryman, W.L., and R.L. Westlake, 1998. A new geographic form of the spinner dolphin, *Stenella longirostris*, detected with aerial photogrammetry, *Marine Mammal Science*, 14(1):38–50.
- Ratnaswamy, M.J., and H.E. Winn, 1993. Photogrammetric estimates of allometry and calf production in fin whales, *Balaenoptera physalus*, *Journal of Mammalogy*, 74(2):323–330.
- Rhineland, M.Q., and S.M. Dawson, 2004. Measuring sperm whales from their clicks: Stability of interpulse intervals and validation that they indicate whale length, *Journal of the Acoustical Society of America*, 115(4):1826–1831.
- Rowe, L., and S. Dawson, 2008. Laser photogrammetry to determine dorsal fin size in a population of bottlenose dolphins from Doubtful Sound, New Zealand, *Australian Journal of Zoology*, 56(4):239–248.
- Shortis, M.R., E.S. Harvey, and D.A. Abdo, 2009. A review of underwater stereo-image measurement for marine biology and ecology applications, *Oceanography And Marine Biology An Annual Review* 47 (R.N. Gibson, R.J.A. Atkinson, and J.D.M. Gordon, editors), CRC Press-Taylor & Francis Group, Boca Raton, Florida, pp. 257–292.
- Spitz, S.S., L.M. Herman, and A.A. Pack, 2000. Measuring sizes of humpback whales (*Megaptera Novaeangliae*) by underwater videogrammetry, *Marine Mammal Science*, 16(3):664–676.
- Willmott, C.J., S.G. Ackleson, R.E. Davis, J.J. Feddema, K.M. Klink, D.R. Legates, J. O'Donnell, and C.M. Rowe, 1985. Statistics for the evaluation and comparison of models, *Journal of Geophysical Research*, 90(C5):8995–9005.

(Received 26 January 2011; accepted 29 April 2011; final version 24 August 2011)